

Sensors and Features Selection for Robust Gas Concentration Evaluation

D. Ahmadou, E. Losson, M. Siadat and M. Lumbreras
Université de Lorraine, LCOMS, EA 7306, Metz, F-57000, France

Keywords: Gas Sensor Properties, Feature Comparison, Derivative Signal, Exposure and Purge times, Drift.

Abstract: This paper seeks to highlight the importance of the knowledge of metal oxide gas sensor behaviour before conceiving an electronic nose for a dedicated application. Therefore, a depth study of sensor response properties is needed for the selection of the more appropriate sensors via optimized measurement conditions and extracted features. Especially for continuous gas evaluation, the most important aspects to consider are the measurement time and the drift of the gas sensors. In this work, for fast recognition of pine oil vapour dilutions, the performance of two features are shown: the maximum of the derivative curve (Peak), an unusual feature which needs a very short gas exposure time, and the sensor amplitude voltage (V_s-V_0) obtained at the end of the gas exposition phase. The performance of the new feature Peak, validated by Principal Component Analysis results, leads us to work with the shortest gas exposition and sensor regeneration times, and allows us to choose the best sensors according to our application.

1 INTRODUCTION

Nowadays, electronic noses gain interest as general purpose detectors of vapours in many fields of application because these mobile and intelligent instruments, easy to build, offer the possibility of direct measurement (Falasconi et al., 2005; Cho et al., 2008; Zhang and Wang, 2007). These systems are largely used to detect, identify or quantify complex atmospheres (Boilot et al., 2002; Branca et al., 2003; Martin Negri and Reich, 2001). They employ an array of gas sensors with different selectivities, more often resistive metal oxide sensors (Gutierrez-Osuna, 2002). The indisputable advantages of these sensors are their high sensitivity, robustness, and commercial availability. But two main limitations must be taken into account to provide fast and reliable gas identification: the delay of the sensor response time and the gas sensor drifts. So, the key requests of electronic noses, working in continuous checking, are the conception of an accurate sampling unit (Roussel et al., 1999) with optimization of the recognition speed.

Considering the electronic nose as a “black box” and referring only to the mathematical computing results after recognition analysis cannot permit robust real-time measurements. Therefore, the entire

knowledge of the gas sensor behaviour is very important to select, for a given application, the best measurement conditions, the best extracted features and the best sensors by considering their characteristics. This selection must be valid for the entire chosen application.

For this purpose, reliable informative features must first be selected to characterize the sensor time-response. This feature selection should take into account the behaviour of the gas sensors for all the studied atmospheres. A lot of features have been mentioned and compared in the literature (Llobet et al., 2002; Distant et al., 2002; Paulsson, 2000; Zhang et al., 2007). Representative features can be extracted either from the transient phase (initial slope, FFT and wavelet descriptors, integral,...) or from the steady-state phase (absolute, relative, fractional or log sensor conductance values) of the sensor time-responses. In the case of steady-state response, obtaining robust features needs generally a long gas exposition time, not suitable for fast recognition system.

We have particularly investigated a novel transient parameter, deduced from the derivative curve of the sensor time-response: the height of its maximum (Peak), occurred before 100 seconds after the gas exposition. The second studied feature is the traditional relative change (V_s-V_0), representing the

sensor response amplitude.

In this work, our electronic nose application concerns the quantification of pine Essential Oil (EO) vapours diluted in pure air. At first, the analysis of the two features (Vs-V0) and Peak will be used to optimize the measurement conditions in order to obtain the fastest quantification. For this purpose, discussions will be done about the robustness of the selected features using the optimized measurement protocol. After this first step, sensors can be characterized by comparing our two features: (Vs-V0) and Peak. The performance of these features will be discussed along with the EO concentrations and the sensor types. Finally, the choice of experimental and calculation conditions, validated by PCA, will allow us to identify the more adequate sensors for our quantitative application.

2 MATERIALS AND METHODS

The study presented in this work concerns an application for the estimation of EO vapour dilutions by using a metal oxide gas sensor (MOX) array. The global aim is to develop an electronic nose based system to regulate the EO diffusion in a closed and conditioned box.

2.1 Equipment Description

A test bench is mounted to generate various EO concentrations in order to characterize and to optimize the commercial MOX array of our electronic nose. Figure 1 presents the functional diagram of this experimental system.

The EO generation is made by bubbling synthetic air flow in a bottle containing 1cm³ of liquid essential oil. To produce a desired EO diluted atmosphere at a constant total flow rate, the created odorant atmosphere is combined with pure air, and then introduced into the gas sensor cell. So, various concentrations are obtained by varying the flow rate of the EO line to be combined with the pure air flow rate. These EO concentrations (dilutions) are then expressed as a percentage of the bubbling flow rate in liquid oil over the total flow rate (100ml/min).

Pine oil at very low percentages (1, 2, 3, and 4%) is utilized in this study. These concentrations correspond to a pleasant odour (human panel) for aromatherapy uses (Sambemana, Siadat and Lumberras, 2010). Gas chromatography measurements were made on the EO pine samples before the beginning and during the experiment phase in order to control the stability of the EO

sample composition (molecules and their concentrations).

The gas sensor cell contains 9 sensors (TGS2620, TGS880, TGS822, TGS816, SPAQ1, SPMW0, SP31, MQ3, MQ138) from Figaro, FIS and Hanwei companies. Sensor responses are digitalized and collected using a fast and high resolution data acquisition board. The whole system will be optimized for an accurate and rapid EO concentration evaluation. In the functional diagram (figure 1), we present also a sensor time-response in terms of sensor voltage response versus time. The signal shows first a voltage increase with an inflexion point, corresponding to the gas exposition. The second part corresponds to the sensor regeneration.

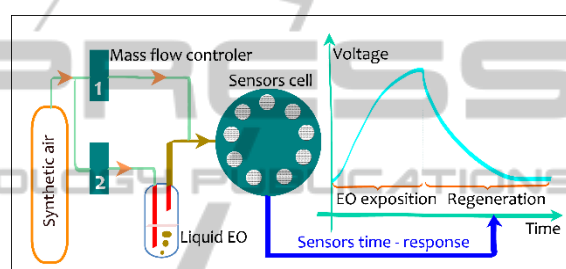


Figure 1: Functional diagram of the gas sensor characterization system.

2.2 Feature Determination

After each gas exposition, a sensor regeneration must be undertaken to recover the conductance basis value of the sensor. In previous studies, we used a cycle composed of 5 minutes gas exposition time followed by 20 minutes regeneration time. This cycle allowed to obtain sensor response stabilization during the exposition phase for all the sensors and all the EO concentrations, and also a good regeneration at the end of the purge phase.

We have tested many characteristic parameters corresponding to transient and steady-state phases (Szcurek and Maciejewska, 2012; Gualdron et al., 2004), and then selected for this study two features: one extracted from the sensor time-response, and the second from the derivative curve of this response.

We have compared the performance of these two features to discriminate the EO concentrations in order to choose the best sensors acting with the shortest measurement cycle, necessary for a real time application.

2.2.1 Derivative Feature

To have a rapid evaluation of the gas concentration,

it is necessary to consider the transient phase of the sensor time-response (Ionescu, Vancu and Tomescu, 2000; Martinelli et al., 2003; Pardo and Sberveglieri, 2007). More we wait for a complete stabilization, more the exposition time is long, and longer will be the regeneration time. In our application, for several studied cases (towards the sensors and/or the gas concentrations) the time-response needs more than 5 minutes to reach 90% of the stabilization level.

The most studied transient feature is the initial slope of the time-response signal (Sysoev et al., 2007; Delpha, Siadat and Lumbieras, 2001). But the difficulty is to determine the starting and the end points of the linear transient phase. It is impossible to fix a general rule for the calculation of this slope because these points vary along with the gas concentration and the sensor types.

So, we have decided to differentiate all the signal time-responses in order to determine the maximum of the derivative curve corresponding to the inflexion point of the sensor time-response. To reduce noise in the derivative signal, it was needed the use of an adapted filtering. Several approaches were tested as Butterworth low pass filtering, Savitzky-Golay (S-G) derivative and smoothing filter, and polynomial fitting (Savitzky and Golay, 1967).

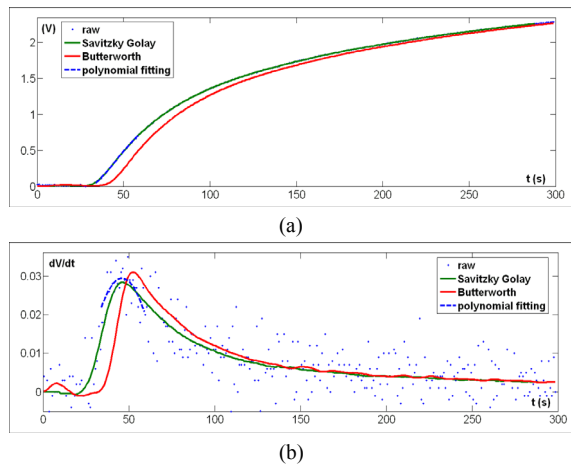


Figure 2: Raw and filtered time-response signals of a gas sensor (a) and their respective derivative curves (b) : Peak apparition in the derivative curve.

The best results were obtained with S-G filter. For each sensor, filter parameters (window width and filter order) were adjusted whatever the used concentration. Figure 2b underlines a notable maximum of the derivative curve, obtained after using an adequate filtering. This peak appears generally in the 75 first seconds, and the height

value depends on the applied gas concentration and the studied sensor.

In Figure 3 we present the derivative curves of the 9 sensors for all the used concentrations. On this figure the four concentrations are represented using different colours. For the gas sensors (except MQ3 sensor), the peak height varies clearly with the concentration. For MQ3 sensor, the superposition of 3% and 4% curves will be explained later.

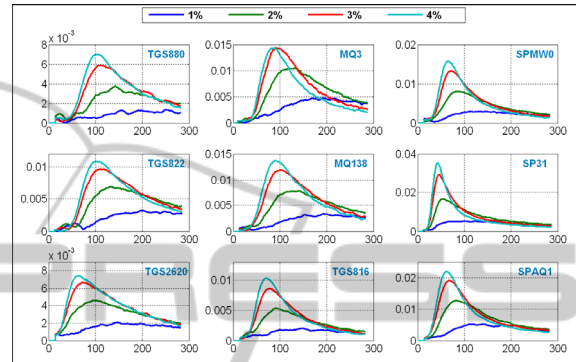


Figure 3: Derivative curves (dV/dt) of each sensor versus exposition time (s) along with the four EO concentrations.

2.2.2 Traditional Features

In most of electronic nose applications the stabilization value of the sensor conductance is used. To compare the Peak feature with this traditional feature, we have determined the $(V_s - V_0)$ parameter where V_s is the sensor response value at the end of the exposure time and V_0 the value of the initial sensor level before the introduction of the EO vapours.

V_s and V_0 values are respectively calculated by averaging five recorded data at the end and the beginning of the sensor time-response signal, in order to reduce the noise effects. The duration of V_0 level is short (about 5 to 10 seconds according to the sensor type) so 5 recorded data are used to average the V_0 value. Concerning V_s , this chosen average gives satisfactory noise reducing.

In Figure 4 the time responses of all the sensors for all the concentrations are drawn. We note that we only obtain a good separation along with the concentration for a few sensors (TGS2620, TGS880, TGS816). The other sensors show high sensitivity to the EO atmospheres than the three first cited sensors with early sensor saturation. So, we see on the corresponding graphs that the saturation occurs from 3% and even from 2% for the MQ3 sensor.

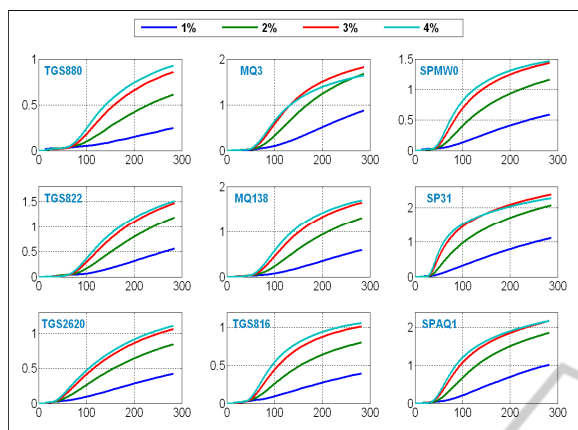


Figure 4: Response signals (V) of each sensor versus exposition time (s) along with the four EO concentrations.

2.2.3 Discussion

The choice of the sensors is predominant for a reliable discrimination with electronic nose systems. We have seen (Figure 4) that the saturation of the sensor time-response occurs unfortunately for many sensors, because of their high sensitivity to the concerned effluent. So, for these sensors the traditional parameter ($V_s - V_0$) cannot well indicate the concentration variation.

Concerning the “transient” parameter, Peak, deduced from the derivative curve, the results (Figure 3) show a better efficiency to discriminate the concentration. In fact, this value is obtained during the transient phase of the sensor time-response (<75 seconds), then it is less influenced by the saturation (excepted for MQ3 sensor).

So, these observations lead us to optimize our detection system by reducing as much as possible the gas exposition time. Consequently this reduction might implicate the regeneration time reduction, taking into account that these two phase times are not linearly related.

This optimization is advantageous in two ways: to reduce the measurement time and to improve the efficiency of the traditional ($V_s - V_0$) feature. This approach will allow us to select the best sensors for our real-time application.

3 MEASUREMENT OPTIMIZATION

In this section we develop the optimization of the measurement protocol, particularly important for real time applications. After discussion about the

choice of the gas exposure and purge times, we insist on the disparity between the sensor behaviours. The study of these disparities permits us to select the best sensors according to the optimized measurement procedure and application.

3.1 Protocol Optimization

We know that measurement cycle has to be composed of the gas exposure phase followed by the sensor regeneration phase. In the considered application, we need to determine the EO concentration as quickly as possible, so one of our goal was to reduce the times corresponding to the measurement and regeneration phases with respect of a good sensor regeneration.

So, several Exposure-Regeneration times were tested. These experiments show us first that, even if the exposure time becomes extremely short (for example 60 seconds), the regeneration time remains still very long (about 300s) to obtain a satisfactory sensor layer cleaning. We have also noted that these times are strongly related to the sensor type and of course, for each sensor they depend on the used gas concentration.

For each value of the studied exposition time, several values of the regeneration time were applied to control the sensor recovery. For an exposition time less than 75s, the sensor time response does not reach either the stabilization value, either the inflexion point. So, it is impossible to determine a reliable value of Peak (maximum of the derivative curve). In contrary, an exposition time of 75 seconds is convenient for all the sensors and most of the pine EO concentrations. We have tested several regeneration times for this exposition time. Figure 5 presents a set of cycles in the cases (a: 75s-150s) and (b: 75s- 350s). In the case (a), all the graphs show an important drift of the sensor initial values. The sensor regenerations are not sufficient. In the case (b), the regeneration is practically obtained for most of the sensors. Other protocol (100s-500s) has given practically the same results than the protocol (75s-350s). This last cycle protocol is adopted for our next investigation. This choice takes into account the importance of a rapid and accurate measurement.

3.2 Sensor Selection

After adopting the measurement protocol, we looked into the matter of the gas sensor selection. As we can see on the Figure 5b, several sensors (TGS816, TGS2620, SPAQ1, SPMW0 sensors) show a good recovery into their initial conductance value after the

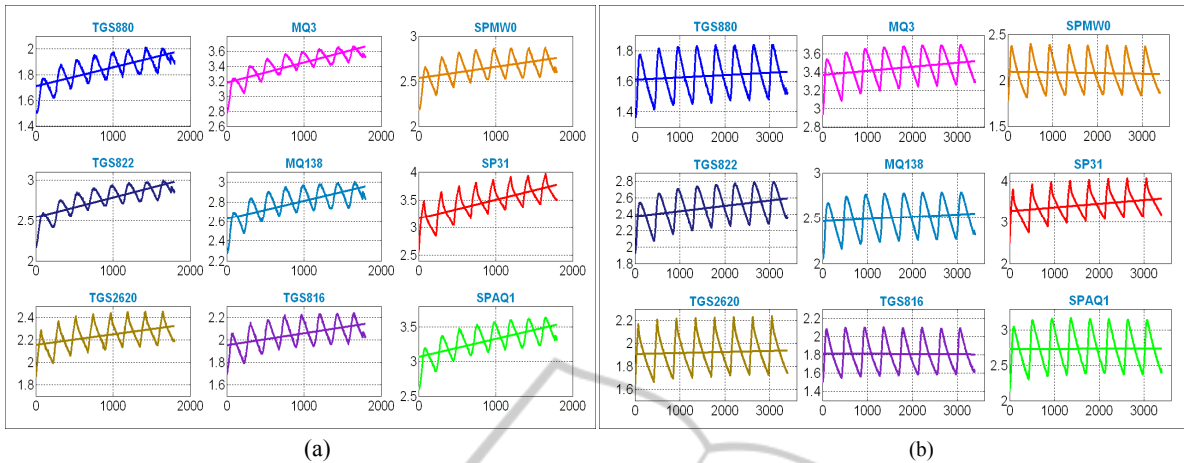


Figure 5: Set of repetitive Exposure-Regeneration cycles for all the sensors and 2% pine oil in the case of (a): 75s-150s and (b) 75s-350s exposure and regeneration times.

regeneration phase. The other sensors present weak or important drift, generally because they give a high response to the EO atmospheres.

As we had characterized nine sensors, we compared the recovery process of each sensor for all the used EO concentrations. For this comparison we have determined the Peak and the (Vs-V0) features. The mean value and the corresponding standard deviation are calculated from all the measurements (8 repetitions), for each sensor and each EO concentration. These values are plotted on the Figure 6 for three representative sensors. We note that the TGS2620 is the more appropriate for pine EO concentrations discrimination: the values of Peak and (Vs-V0) features show a very sensible rise along the EO concentration with weak standard deviations. But we can surprisingly see the inefficiency of the SP31 sensor for this application. Because of its high sensitivity to pine atmosphere, the saturation occurs after 1% EO, represented by abnormal evolution of the (Vs-V0) and Peak values versus EO concentration. For the SPAQ1 sensor the behaviour is intermediate, with a good variation of Peak and a rather less efficient variation of (Vs-V0), essentially higher than 3% EO concentration.

This comparison study leads us to detect three qualities of sensors among our sensor array: very good, good and non-adapted sensors for the concerned protocol and application.

- Very good: TGS 2620, TGS 880, SPMW0
- Good: TGS 816, TGS822, SPAQ1, MQ138
- Non-adapted: SP31, MQ3

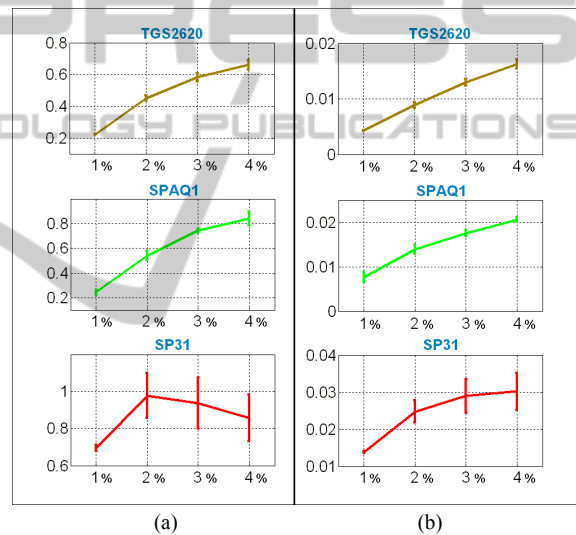


Figure 6: Feature evolutions of 3 gas sensors versus pine EO concentrations (1, 2, 3, 4%); (a) Vs-V0, (b) Peak.

3.3 PCA Results

The measurements made for all the concentration range (1, 2, 3, 4%) were analysed by Principal Component Analysis (PCA) using as explicative variables one of the two selected features (Peak or (Vs-V0) of the nine sensors) separately. So, nine principal components are obtained by linear combinations of the original variables and participate decreasingly to the construction of the model. Figure 7 shows on the first two principal components (PC1 and PC2) the loadings plots of each of the two variable sets. A loading plot present the correlation between the concerned variables, so

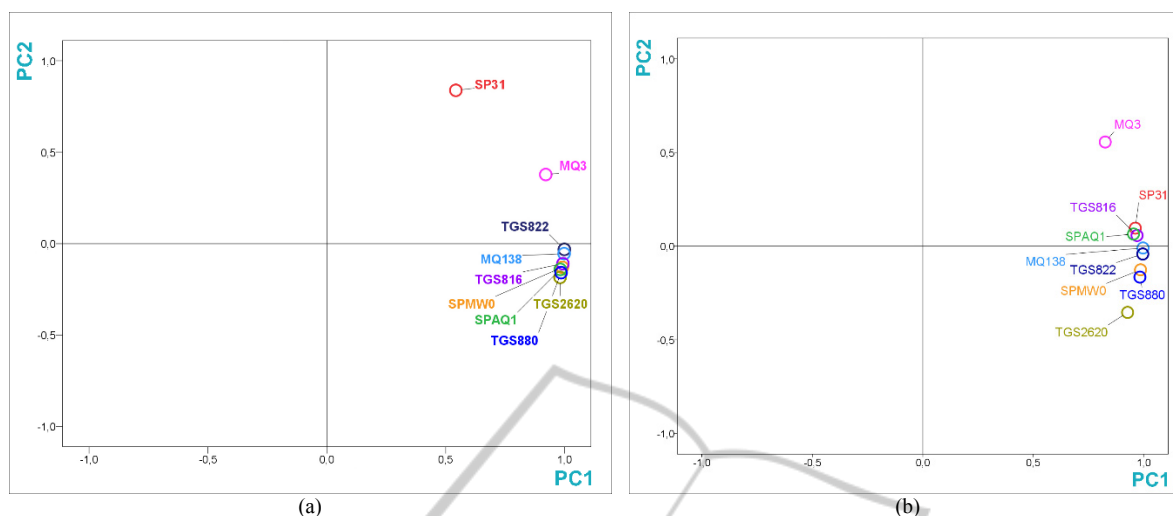


Figure 7: PCA loading plots; (a) Vs-V0 with PC1 explaining 88.9% of the variation and PC2 10.6%; (b) Peak with PC1 explaining 91.6% of the variation and PC2 5.5%.

all the representative points are positioned inside a unit length circle, called “circle of correlation”.

In our case, each variable characterises one of the nine gas sensors. So, the loading plot, given by PCA, provides a map of how the sensors relate to each other. In this map, the more sensor projections are closed together, the more they present similar properties. Furthermore, the distance to the origin of PC1 and PC2 also conveys information: the further away from the plot origin a variable is located, the stronger impact that variable has on the model with respect of the EO concentration separation. The more a variable is close to the origin of the plane, the less important it is (Berna, Anderson and Trowell, 2009; Jolliffe, 2002). In the same way, since the PC1 explains the most important part of the variation than PC2, this impact is stronger when the variable is near to the unit length of PC1.

In Figure 7(a), where (Vs-V0) feature of each sensor is used as representative variable, we can note that SP31 and MQ3 sensors are situated far from the unit length of the PC1. They are then less adapted than the other sensors. This observation confirms the previous result about the efficiency of these two sensors. Other sensors of the array are positively correlated and satisfy the condition of strong impact.

Considering Figure 7(b) where Peak is used as representative feature, we can observe that the SP31 sensor becomes more efficient and joints other group of sensor with high impact. But MQ3 sensor is definitively less adapted for this study.

These PCA results confirm our sensor behaviour study (section 3.2).

4 CONCLUSIONS

We have shown through this work that a deep evaluation of the sensor behaviour according to the studied atmosphere is required for reliable electronic nose application such as gas quantification. Two features extracted from the transient and the steady-state phases of the sensor response signal (Peak: the maximum of the derivative signal of sensor response, and (Vs-V0): the response amplitude voltage) were studied and compared. The performance of the unusual Peak feature is highlighted to provide fast and continuous measurement. The capacity of this feature to quantify pine oil vapour diffused in pure air has permitted the optimization of the measurement time conditions and also the selection of the best sensors. In fact we have shown important disparities on the stability and the performance of the chosen features along with the sensor types. Loading plots obtained with PCA confirm these results.

REFERENCES

Berna, A. Z., Anderson A. R., Trowell S. C., 2009. Bio-Benchmarking of Electronic Nose Sensors. *PLoS ONE*, 4(7): e6406; [Online]; doi: 10.1371/journal.pone.0006406.
 Boilot, P., Hines, E. L., Gongora, M. A., Folland, R. S., 2002. Electronic noses inter-comparison, data fusion and sensor selection in discrimination of standard fruit solutions. In *Sensors and Actuators B*, 88, 80-88.

- Branca, A., Simonian, P., Ferrante, M., Novas, E., Martin Negri R., 2003. Electronic based discrimination of a perfumery compound in a fragrance. In *Sensors and Actuators B*, 92, 222-227.
- Cho, J. H., Kim, Y. W., Na, K. J., Jeon G. J., 2008. Wireless electronic nose system for real-time quantitative analysis of gas mixtures using micro-gas sensor array and neuro-fuzzy network. In *Sensors and Actuators B*, 134, 104-111.
- Delpha, C., Siadat, M., Lumbresas, M., 2001. An electronic nose using time reduced modelling parameters for a reliable discrimination of Forane 134a. In *Sensors and Actuators B*, 77, 517-524.
- Distante, C., Leo, M., Siciliano, P., Persaud, K.C., 2002. On the study of feature extraction methods for an electronic nose. In *Sensors and Actuators B*, 87, 274-288.
- Falascioni, M., Pardo, M., Sberveglieri, G., Ricco, I., Bresciani, A., 2005. The novel EOS⁸³⁵ electronic nose and data analysis for evaluating coffee ripening. In *Sensors and Actuators B*, 110, 73-80.
- Gualdrón O., Lobet E., Brezmes J., Vilanova X., Correig, X., 2004. Fast variable selection for gas sensing applications. In *Sensors, 2004. Proceeding of IEEE*, 2, 892-895.
- Gutierrez-Osuna R., 2002. Pattern analysis for machine olfaction: A review. In *IEEE Sensor Journal*, 2, 189-202.
- Ionescu, R., Vancu, A., Tomescu, A., 2000. Time-dependent humidity calibration for drift corrections in electronic noses equipped with SnO₂ gas sensors. In *Sensors and Actuators B*, 69, 283-286.
- Jolliffe, I.T., 2002. *Principal Component Analysis, Second edition*. New York: Springer.
- Llobet, E., Ionescu, R., Al-Khalifa, S., Brezmes, J., Vilanova, X., Correig, X., Barsan, N., Gardner, J.W., 2002. Multicomponent gas mixture analysis using a single tin oxide sensor and dynamic pattern recognition. In *Sensors Journal, IEEE*, 1 (3), 207-213.
- Martin Negri R. and Reich S., 2001. Identification of pollutant gases and its concentrations with a multisensory array. In *Sensors and Actuators B*, 75, 172-178.
- Martinelli, E., Falconia, C., D'Amico A., Di Natale, C., 2003. Feature Extraction of chemical sensors in phase space. In *Sensors and Actuators B*, 95, 132-139.
- Pardo, M. and Sberveglieri, G., 2007. Comparing the performance of different features in sensor arrays. In *Sensors and Actuators B*, 123, 437-443.
- Paulsson, N., Larsson, E., Winquist, F., 2000. Extraction and selection of parameters for evaluation of breath alcohol measurement with an electronic nose. In *Sensors and Actuators B*, 84, 187-197.
- Roussel, S., Forberg, G., Grenier P., Bellon-Maurel, V., 1999. Optimisation of electronic nose measurements. partII: Influence of experimental parameters. In *Journal of Food Engineering*, 39, 9-15.
- Sambemana, H., Siadat, M., Lumbresas, M., 2010. Gas sensing evaluation for the quantification of natural oil diffusion. In *Chemical Engineering Transaction*, 23, 177-183.
- Savitzky, A. and Golay, M.J.E., 1967. Smoothing and Differentiation of Data by Simplified Least Squares Procedures. In *Anal. Chem.*, 36 (8), 1627-1639.
- Sysoev, V. V., Goschnick, J., Schneider, T., Strelcov, E., Kolmakov, A., 2007. A gradient microarray electronic based on percolating SnO₂ nanowire sensing elements. In *Nano letters*, 7 (10), 3182-3188.
- Szczurek, A. and Maciejewska, A., 2012. Gas Sensor Array with Broad Applicability, Sensor Array, Prof. Wuqiang Yang (Ed.), ISBN: 978-953-51-0613-5, InTech. Available from: <http://www.intechopen.com/books/sensor-array/gas-sensor-array-with-broad-applicability>.
- Zhang, S., Xie, C., Zeng, D., Zhang, Q., Li, H., Bi, Z., 2007. A feature extraction method and a sampling system for fast recognition of flammable liquids with a portable E-nose. In *Sensors and Actuators B*, 124, 437-443.
- Zhang, H. and Wang, J., 2007. Detection of age and insect damage incurred by wheat, with an electronic nose. In *Journal of Stored Products Research*, 43, 489-495.